International Journal of Thermophysics, Vol. 24, No. 2, March 2003 (© 2003)

Dynamic Low-Frequency Electrical Impedance of Biological Materials Subject to Freezing and Its Implementation in Cryosurgical Monitoring

T. H. Yu,[1] Y. X. Zhou,[1] and J. Liu[1,2]

Received October 3, 2002

A precise monitoring of the extent of freezing during a cryosurgical process has been an important problem in health-care clinics. Among various existing techniques, the dynamic electrical impedance utilizing the impedance jump to detect the ice moving front, is a suitable way because the impedance of frozen tissue is much higher (3 to 4 orders of magnitude or even larger) than that of unfrozen tissue. Based on two experimental setups, the dynamic low-frequency impedance (DLFI) and impedance changing rate (ICR) for selected biological materials (fresh pork and rabbit tissues) subject to freezing were systematically measured. Their transient behaviors were investigated, and implementations in a practical cryosurgery to detect ice front propagation were analyzed. Furthermore, *in vitro* experiments were performed on distilled water and phantom gel. The experimental results, obtained with a two-electrode measuring technique, are as follows: (1) The impedance of all samples has a rapid response to the external freezing. (2) The impedance will not jump into an insulation region when the cooling temperature is not low enough. (3) As an alternative to DLFI, ICR imaging can also give important information for the phase-change process, which may lead to an efficient method to detect the ice-ball growth. (4) There is an evident variation in DLFI for different biological tissues when subjected to the same cooling temperatures; this value also differs for the same tissue under different cooling conditions.

KEY WORDS: biological material; cryosurgery; DLFI; ice front propagation; ICR; Impedance; phase change.

[1] Cryogenics Laboratory, P.O. Box 2711, Technical Institute of Physics and Chemistry, Chinese Academy of Sciences, Beijing 100080, People's Republic of China.
[2] To whom correspondence should be addressed. E-mail: jliu@cl.cryo.ac.cn

0195-928X/03/0300-0513/0 © 2003 Plenum Publishing Corporation

1. INTRODUCTION

Biological materials can be either preserved or destroyed during the process of a freezing. Investigations in this area have led to many important applications in health-care clinics. Freezing properties have been found important in tissue preservation (cryopreservation) or cancer treatment (cryosurgery) [1]. With an understanding of the relationship between the electrical characteristics of a tissue and its biological/physiological parameters, impedance measurements have been an important evaluation method of tissue behaviors [2, 3]. They can give useful information on tissue structures and their physiological states and functions [4]. The electrical impedance of biological tissues varies by orders of magnitude as a result of their diverse electrical properties, e.g., the permeability of the cell membrane, ionic concentration, etc. For example, the impedance for cerebrospinal fluid is about 65 $\Omega \cdot$m, for blood 150 $\Omega \cdot$m, for lung tissue between 700 and 2100 $\Omega \cdot$m, and for bone 16,600 $\Omega \cdot$m [5]. In recent years, the bio-electrical impedance has been applied in many medical diagnoses and examinations [6–9], most of which are related to global information about the body or the biological system. This paper is aimed at investigating the role of impedance measurements as a tool of monitoring cryosurgery.

Cryosurgery is a surgical technique that employs freezing to destroy undesirable tissues. Applications of this technique are quite wide including the treatment of hemorrhoids, glaucoma, and malignant tumor [10]. Cryosurgery is usually performed with a cryoprobe, which is cooled internally with a cryogen and insulated at the outside wall. The probe is placed in contact with the tissues to be treated. As heat is removed, a freezing interface propagates through the tissue from the probe surface [11]. One of the major difficulties encountered in cryosurgery is the uncertainty of the freezing extent of the tissues treated. The real-time imaging techniques to monitor the moving ice front are thus important for the successful operation of cryosurgery. Failure to evaluate this information correctly can lead to either insufficient or excessive freezing and, consequently, to recurrence of malignancies or destruction of healthy tissues.

During the late 1970s, several researchers, the first of whom were Pivert and his colleagues [10], suggested the use of local electrical impedance measurements to monitor cryosurgery. It was shown that as tissue, which is essentially a solution of electrolytes, becomes frozen, its impedance increases from several kilohms in living tissues to several megohms in frozen tissues [12–14]. General impedance measurements are based on detecting the extent of freezing through direct measurements of electrical potentials at discrete positions inside the tissues, with electrodes placed inside or around the undesirable tissue that is being frozen. Different from

other monitoring techniques such as computed tomography [15], ultrasound [16], magnetic resonance imaging [17], acoustic impedance, and nuclear spin phenomena, electrical impedance tomography (EIT), as a relatively young imaging technique, is recognized as a cheap and noninvasive cryosurgical monitoring technique. Despite its typically limited spatial resolution, EIT offers portability, fast image acquisition, and no dosage concerns in a relatively inexpensive way [2, 10]. A number of groups have thus previously explored impedance measurements as a means to monitor cryosurgery with local electrode placement.

To better understand the transient behavior of the DLFI of biological materials subjected to freezing and to further demonstrate the feasibility of the noninvasive bioimpedance technique for monitoring cryosurgery, the goal of this paper is focused on measurements of the DLFI of biological materials under various cooling situations. For this purpose, we have designed and constructed a basic measurement system and a sample chamber with temperature controlling capability to produce a precisely known temperature inside the biological material. For the low frequencies applied in these experiments, the capacitance components of electrical impedance can be neglected. With this simple, low-frequency bio-impedance measurement system, two planar electrodes are used to detect the change in impedance due to the presence of a freezing front under a specific cooling temperature. We also developed a cryoprobe to examine the practical application of DLFI, and *in vitro* freezing experiments on distilled water and phantom gel were completed. Some approaches were particularly suggested for the monitoring of a practical cryosurgery.

2. EXPERIMENTAL SETUP

2.1. Sample Chamber

From the preliminary feasibility studies [18], a four-electrode system is usually used to measure the bio-electrical impedance. The potential distribution develops as a result of current flow, and hence the measured surface potentials are not only a function of the impedance distribution, but also of the geometry of the medium and of the position of the measurement electrodes relative to the current inserting electrodes. The four-electrode system appears to have disadvantages to detect the DLFI; therefore, two planar copper electrodes shown in Fig. 1 have been selected as the measurement configuration. The electrical current can flow between the two electrodes that also serve as the flat interface for transferring heat. The biological material is placed between the two copper electrodes whose sizes are $30\ \text{mm} \times 25\ \text{mm} \times 0.2\ \text{mm}$. Then they are sandwiched between two glass

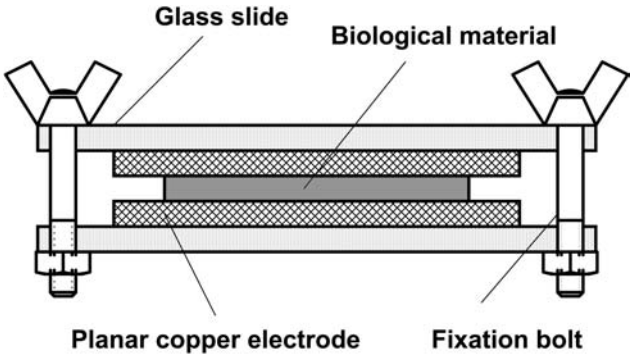

Fig. 1. Schematic of sample chamber.

slides fixed by bolts for better contact. This configuration for the sample chamber not only firmly holds the biological material and the copper electrodes, but also allows the sample chamber to move easily up and down, which is to control the sample temperature in the liquid nitrogen container. Also, two copper-constantan thermocouples are used to monitor the temperatures in the sample chamber. One is inserted into the center of the biological material to measure its temperature; another is mounted on the surface of a glass slide to monitor the surrounding nitrogen gas temperature.

2.2. Cryoprobe

The cryoprobe used in the present *in vitro* experiments was designed and fabricated with a standard Linde style [19]. The probe consists of three concentric stainless-steel tubes arranged as shown in Fig. 2. Upon activation, liquid nitrogen flows from a pressurized supply source through the inner tube. It ultimately reaches the hemispherical probe tip. Small holes (0.3 mm diameter) are drilled at the exit of the inner tube to allow liquid nitrogen to run into the probe tip filled with copper silk, which is to

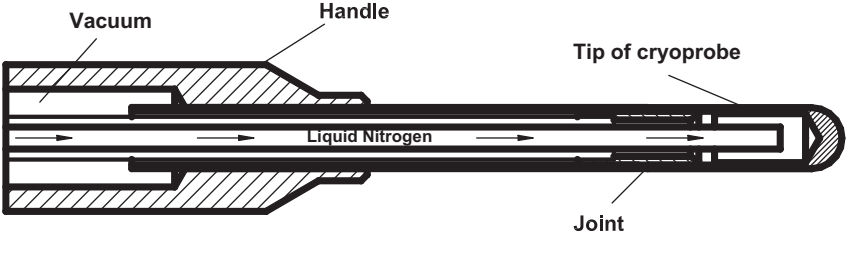

Fig. 2. Structure of the cryoprobe and flow path of the working fluid.

enhance heat transfer. The annulus formed between the inner tube and the middle tube allows the nitrogen vapor to escape to the environment. The outermost annulus is evacuated, with the aid of a vacuum pump, which is to provide thermal insulation along the probe wall [20]. In this study, the diameter of the prototype probe was designed as 5 mm. The temperature of the probe tip is a function of the flow rate of liquid nitrogen, which is manually adjusted to obtain the desired tip temperature. In our experimental setup, a copper-constantan thermocouple is welded on the probe tip to monitor its temperature. Figure 3 shows the picture of an ice ball formed around this cryoprobe. The typical size for a produced ice ball is about 30 mm × 25 mm.

2.3. DLFI Measurement System

In this study, a new apparatus and experimental procedure have been developed to facilitate a systematic study of the DLFI of biological materials during freezing. The schematic diagram of the apparatus is given in Fig. 4. As we know, the boiling temperature for liquid nitrogen at atmospheric conditions is −196°C and that for the outlet of the Dewar container is approximately at the surrounding temperature (25°C). Thus, the temperature inside the samples and its freezing rate can be easily controlled within a quite broad range by moving the sample chamber up and down. The tissue samples freeze under prescribed thermal conditions, which can be directly correlated with the thermophysical events that the

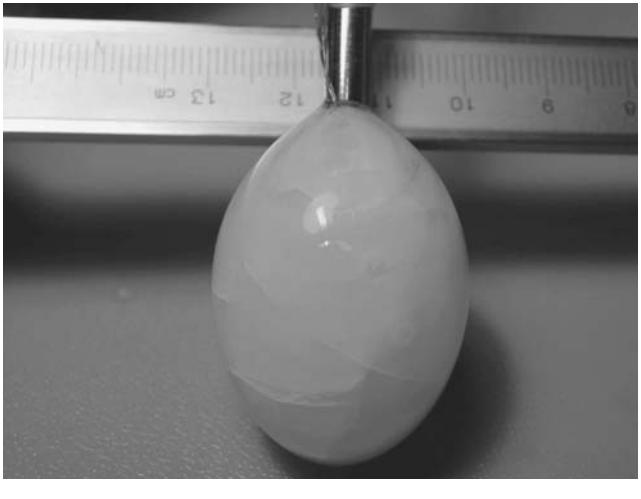

Fig. 3. Photo of an ice ball formed with present cryoprobe.

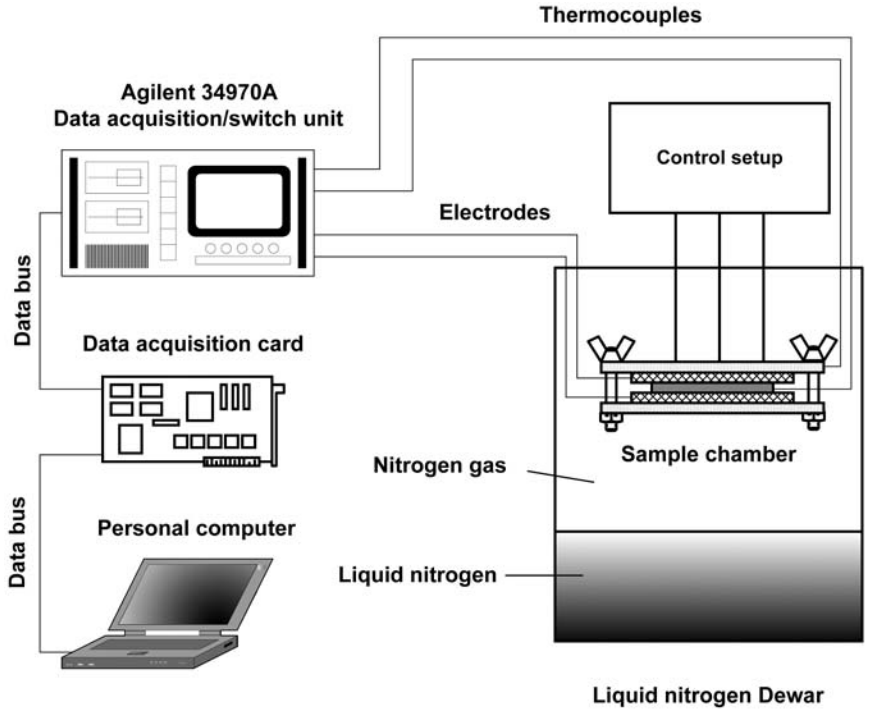

Fig. 4. Schematic diagram of instrument to measure biological material impedance during freezing.

tissue has experienced. The temperatures of nitrogen gas and that inside the material were monitored by two thermocouples.

Several typical biological samples were tested: fresh pork, fresh muscle tissue of rabbit, and fresh organs of rabbit, with 4 to 6 trials for each type. The tissue slices were all taken from the same area of fresh pork, fresh rabbit muscle and organs. For each trial, the biological tissue was sliced to a predetermined size. Then one sample was sandwiched between the two planar copper electrodes, taking care to evacuate all air bubbles with a syringe, and ensuring that good contact was guaranteed at the electrode interface. A short circuit was avoided because the sample size is approximately the same as that of the copper electrodes. After that, the planar electrodes were carefully fixed with two glass slides and bolts to avoid sample transfiguration. Thus, the chamber was finished, and then secured into the Dewar container and connected with electrode leads. When the control setup was engaged and the sample was placed into a desired temperature condition, data logging was started. When the impedance of the

sample jumped to over 100 MΩ (can be regarded as in an insulation region), the sample chamber was taken out of the container. The DLFI of the thawing process was measured. An entire experiment was thus finished and data logging was stopped, when the sample impedance dropped to its normal level.

2.4. Implementation of DLFI in Cryosurgery

To test DLFI as a tool of monitoring cryosurgery, an experimental setup was specially constructed as shown in Fig. 5, which differs from Fig. 4 in that the sample chamber was replaced by a cryoprobe. During a typical experiment, several electrodes were mounted along the exterior of the cryoprobe. The probe, made of stainless steel, was used as the public cathode, and each needle electrode serves as a single anode. In this way, the DLFI caused by ice ball formation during cryosurgery can be easily monitored by these combined needle electrodes: the impedance has a normal level, when no ice ball is formed along the probe, otherwise, it will quickly jump to a high value until the insulation region occurs. In this

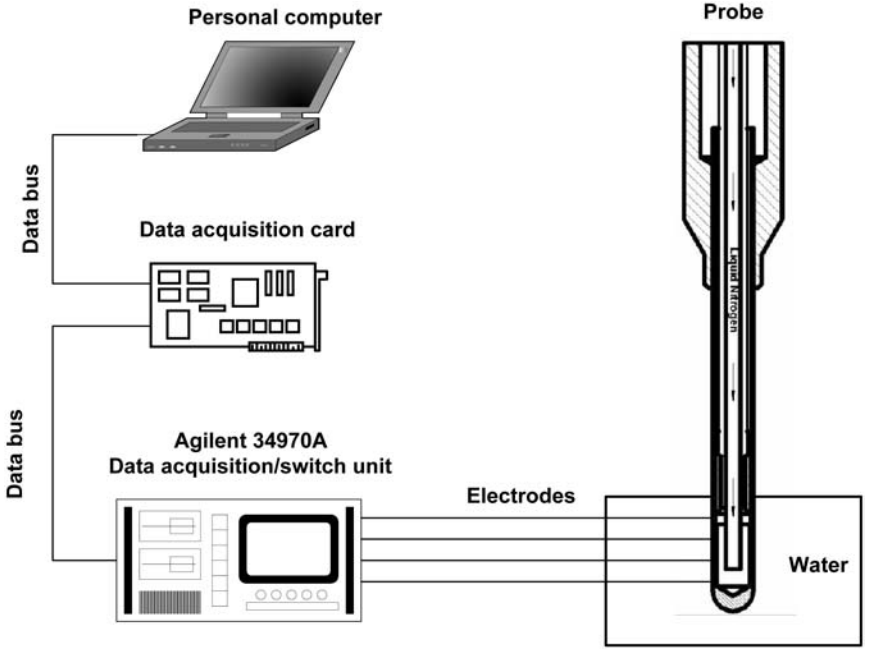

Fig. 5. Schematic diagram of system to examine the implementation of DLFI in a practical cryosurgery.

study, 5 or 6 electrodes have been used for illustration purposes. One is fixed at the tip of a probe while the others are mounted at a distance of 3, 6, 9, 12, and 15 mm from the tip along the probe.

The medium used to simulate the tissue was chosen as a clear gel composed of 10 percent of gelatin and 90 percent of water in volume. The gel can exhibit two highly desirable features as an experimental medium. First, it is almost transparent which is easy to observe. Second, the gel has quite similar properties to that of water, while 80 percent of living tissue is water. At first, the gelatin in the liquid form is contained in an organic glass box, then cooled for about one hour in the refrigerator until the liquid changes to solid. When the gel was left in the air to be completely warmed at a relatively uniform room temperature, it would be ready for use. Then, the probe was vertically inserted into the distilled water and phantom gel and positioned with a special brake. Once the electrode circuit was turned on, the coolant inside the cryoprobe was supplied and data acquisition began. After about 1 minute, the liquid nitrogen came to the probe tip and an ice ball began to form. The lowest temperature of the probe tip was about $-80°C$ in our experiments. When the ice ball stopped growing, the pressurized coolant supply was shut off. Then, after several minutes, the ice ball around the probe tip disappeared and the entire freeze-thaw cycle was finished. Detailed measurements on the impedance jump will be reported in a later section

2.5. Data Acquisition System

In our experiments, the impedance and temperature data for each sample were obtained using a 48-channel HP Agilent 34970 Data Acquisition/Switch Unit. The working current for the 100 MΩ range is 500 nA in the DLFI experiments. The thermocouples were calibrated in ice water, and an uncertainty of $\pm 0.1°C$ was obtained. The multimeter is connected to a personal computer with an HP-IB interface (IEEE-488) and a data acquisition card (HP E2078A, USA). The acquisition software uses HP BenchLink Data Logger, which can immediately display, analyze, and save the input measurement data.

3. RESULTS

A typical DLFI response of a biological material due to freezing is shown in Fig. 6. The measured sample was a fresh pork with a size $30\,mm \times 20\,mm \times 2\,mm$, and the temperature for the surrounding cooling nitrogen gas is at about $-100°C$. From this figure, it is clearly shown that the temperature inside the sample begins to decrease, once the sample

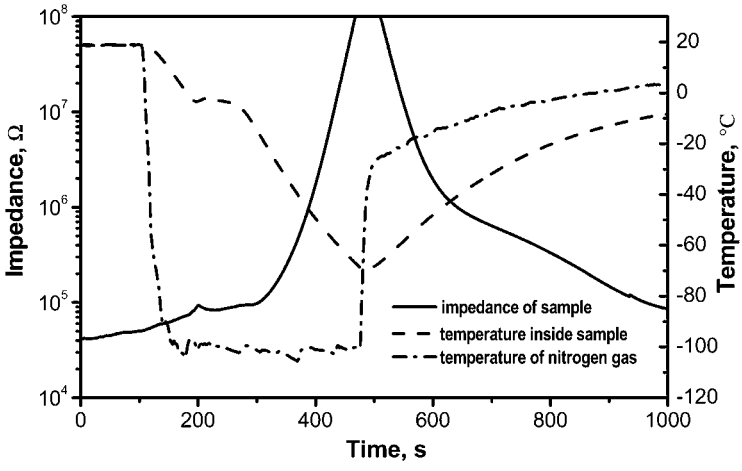

Fig. 6. Typical impedance jump of biological material, fresh pork with a size of 30 mm × 20 mm × 2 mm under −100°C.

chamber is immersed into the Dewar. When the sample temperature drops to about 0°C, it stays there for several seconds. Over this period, the impedance increases slowly. Once the temperature inside the sample decreases again, the impedance will quickly increase to be over 100 MΩ, which can be regarded as that of an insulation material.

The physical view of the ice formation process can explain the above phenomenon. When the sample was frozen at about 0°C, the ice crystal first comes into form. Considering the occurrence of nucleation, ice will have a higher probability of forming in the extracellular region, which has a larger volume than the highly compartmentalized cells. Therefore, when the tissue is frozen, the ice begins to form and propagate though the extracellular environment, while the water in the cells remains in a supercooled state. The temperature stays constant over this period, after which the impedance increases will become much quicker, as indicated in Fig. 6. It is assumed that intracellular crystallization then begins to occur. For a high cooling rate, crystallization of water in the cells can be initiated in a shorter time and it becomes sufficiently supercooled for intracellular ice to form prior to complete dehydration. Then the impedance will keep increasing until its magnitude is over the measurable range of the current apparatus. From the view of the freezing mechanism, the extracellular and intracellular crystallization can both cause damage to cells, because of the dehydration of cells and volume accretion of cells (the density of ice is larger than for water). In a previous study, other damage mechanisms were also proposed such as denaturation of proteins in the dehydrated cells, the

process of recrystallization, and the mechanical damage to cell membrane under the pressure of extracellular crystallization [21].

Once the impedance is out of the measurable range, the sample chamber was removed from the Dewar container. It will be left in air to warm up, and the thawing process thus begins. From Fig. 6, the impedance of the sample decreases quickly at the beginning of thawing. This trend was slowed down when the impedance gets back to its normal level. This experimental phenomenon can be explained by analyzing the process of ice melting. The majority of melting ice at the beginning is in extracellular space; therefore, this melting process is direct and quick. When the temperature inside the biological sample is about −40°C, the water is transported through the semi-permeable cell membrane and begins to melt the intracellular ice. Therefore, this melting process will be much slower.

Figures 7 and 8 represent the overall impedance changing rate (ICR) and part of the ICR of the typical impedance jump for biological materials, respectively. Compared with Fig. 6, which displays the impedance values, the ICR appears better to reveal the essence of the impedance change. As shown in Fig. 7, the ICR begins to increase with high gradients when the temperature inside the sample drops to −50°C. The highest value for the ICR occurs at the time of reaching an insulation level and when rewarming begins. However, in Fig. 7, the details of the ICR over most of the period of time are not available, because the values are much smaller than that for reaching the insulation level. Thus, a special period of time was re-displayed as in Fig. 8, in order to investigate the impedance change during the

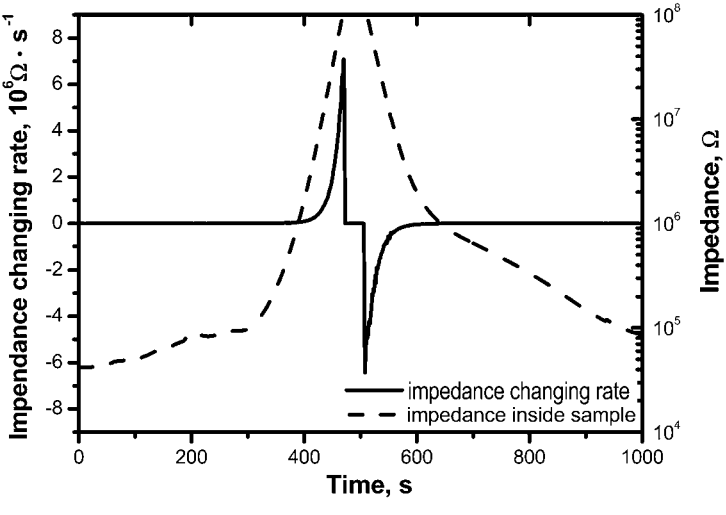

Fig. 7. Overall ICR of typical impedance jump of biological material.

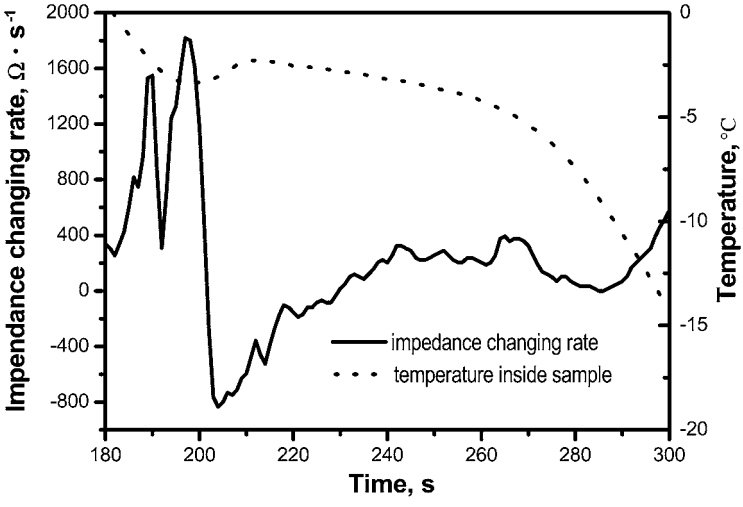

Fig. 8. Partial ICR of typical impedance jump of biological material during phase-change stage.

phase change. From this figure, the temperature inside the sample has a slight increase when it drops to about −4°C. This is because the phase change has occurred and crystallization released a certain amount of heat. At that time, it is found that the ICR quickly decreases until it becomes negative (about $-800\,\Omega\cdot s^{-1}$). The same result was also obtained in other experiments for which the ICR shows an evident decrease to a negative value when super-cooling begins. This implies that the increasing rate of impedance slows, and even becomes negative at the early stages of the phase change. This result can be explained by analyzing the relation of crystallization and damage of cell. The ice is formed when the temperature is low enough, which can cause an impedance increase. Besides, the sharp ice crystal can possibly thrust through the cell membrane; thus, the electrolyte inside the cell flows out, resulting in an impedance decrease.

Figure 9 depicts the impedance jump of a rabbit muscle with a size of 20 mm × 20 mm × 2.5 mm under a surrounding nitrogen gas temperature of −60°C. From this figure, one can observe that the impedance increases rapidly with a decrease of the temperature inside the biological sample. However, it does not jump into the insulation region (i.e., over 100 MΩ) in contrast with Fig. 6. The impedance retains a rather high value and has an oscillation in a small range due to the reciprocal occurrence of crystallization and recrystallization in cells, when the temperature inside the biological sample becomes close to −60°C and remains relatively constant. This phenomenon implies that this biological sample had not been completely

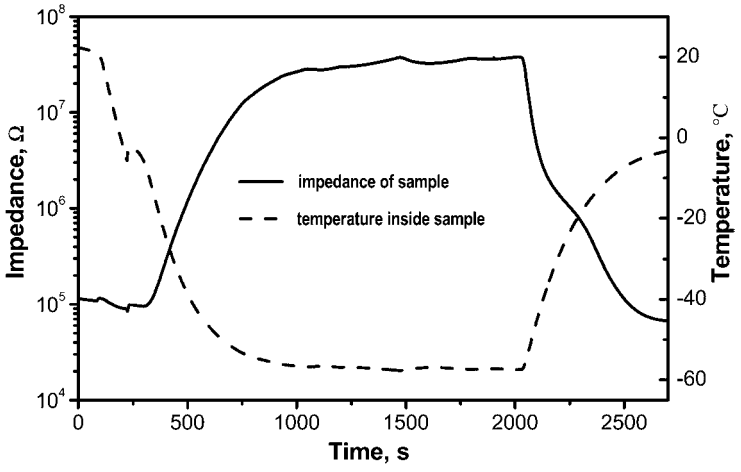

Fig. 9. Impedance change of rabbit muscle with a size of 30 mm × 20 mm × 2.5 mm during freezing (the lowest temperature inside sample is close to −60°C).

frozen, which is beyond our common knowledge. As discussed above, the freezing process initially occurs in the extracellular space and the intracellular crystallization is initiated much later. The unfrozen water in the cell, therefore, experiences greater thermodynamic supercooling. This supercooled intracellular solution is thermodynamically unstable, and after reaching a certain value, nucleation and freezing will occur. Therefore, if the cooling rate is not quick enough, the supercooled intracellular solution will not be frozen [22]. In order to validate this interpretation further, an additional experiment was conducted and the result is shown in Fig. 10. The nitrogen gas temperature was approximately controlled to −60°C and then given a certain perturbation to examine the DLFI. From this figure, the impedance stills stays relatively steady when the sample temperature goes down to −60°C, which is the same as in Fig. 9. Using the control setup, the sample temperature was decreased over a small range. As a result, the impedance begins to increase. If the sample temperature is low enough, the impedance will represent an insulation level. Otherwise, the impedance will also remain steady at a higher value. This experimental results strongly support the interpretation proposed above.

Figure 11 shows the DLFI of different biological tissues of rabbit organ with a size of 30 mm × 20 mm × 3 mm during freezing. The freezing temperature is controlled at −100°C. These organs (liver, muscle, kidney, and heart) are obtained from a rabbit just sacrificed, and the experiments were immediately performed to make sure the tested samples were fresh. It is seen that the DLFI has an evident difference for each kind of tissue. The

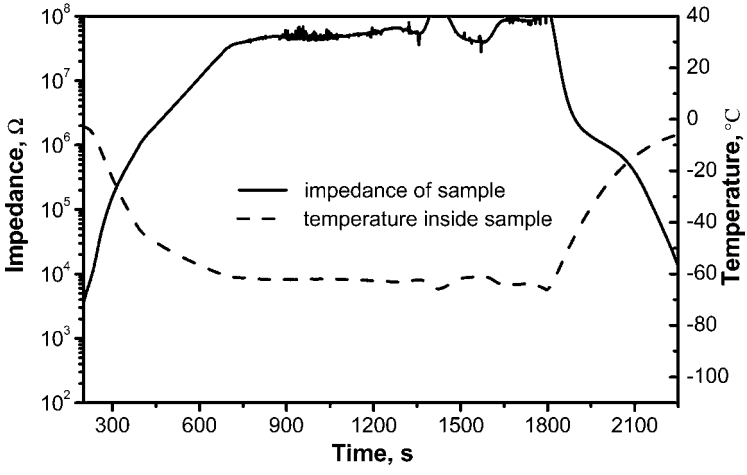

Fig. 10. Impedance change of pork with a size of 30 mm × 20 mm × 1.5 mm during freezing (the lowest temperature inside sample is slightly below −60°C).

impedance of a kidney sample reaches an insulation level most quickly while it is the slowest for a heart sample. The reason may be due to that the DLFI depends heavily on the property of biological tissues, such as the water content, density, proportion of blood vessels, etc. Figure 12 depicts the DLFI of pork with a size of 20 mm × 20 mm × 1.5 mm under two different cooling temperatures (−70 and −100°C). From this figure, the

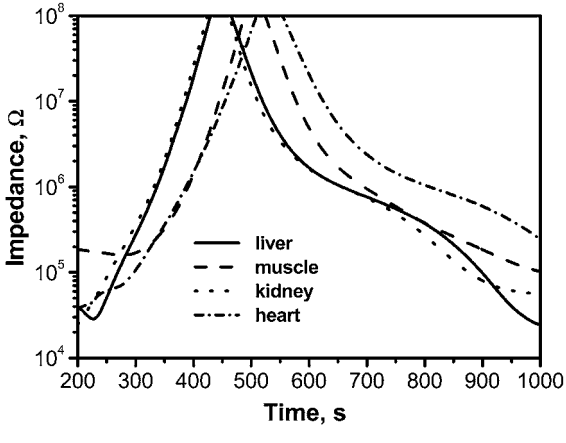

Fig. 11. Impedance change of different biological tissue of rabbit organs with a size of 30 mm × 20 mm × 3 mm during freezing (surrounding nitrogen temperature is −100°C).

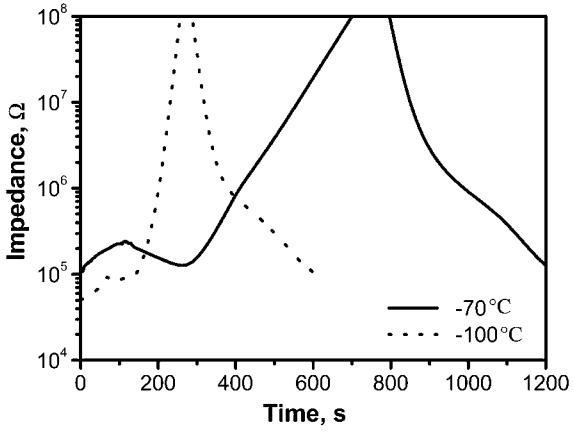

Fig. 12. Impedance change of pork with a size of 20 mm × 20 mm × 1.5 mm at two different nitrogen temperatures (−70 and −100°C).

impedance increases much slower when the cooling temperature is at −70°C rather than at −100°C during freezing. However, the DLFI of the thawing process is approximately the same for both cases. This is because both sample chambers were left in air to warm up after freezing.

The experimental results of implementing the DLFI in cryosurgery are shown in Figs. 13 and 14, and the test mediums are water and phantom gel.

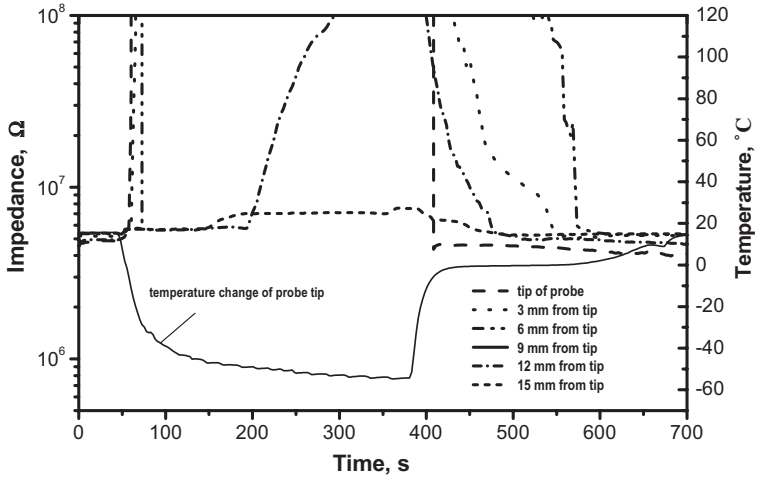

Fig. 13. Impedance jump of probe exterior electrodes and temperature change of probe tip during the water experiment.

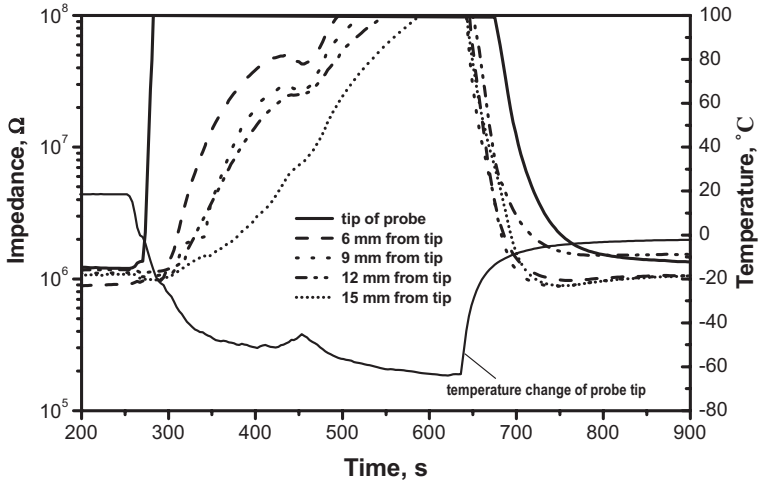

Fig. 14. Impedance jump of probe exterior electrodes and temperature change of probe tip during the phantom gel experiment.

The temperature change of the probe tip is monitored by a thermocouple. In the water experiment, electrodes are mounted at the tip, and at distance of 3, 6, 9, 12, and 15 mm from the tip along the wall of the probe (see Fig. 5). From Fig. 13, it was found that the impedance quickly increases to insulation in a short time at the probe tip and at distances of 3 and 6 mm from the tip, once liquid nitrogen arrived at the probe tip. This result is determined by the configuration of the probe. In this study, the probe is designed as a column. A thin ice layer formed around the exterior of the tip when liquid nitrogen arrived; thus, the electrodes inside the ice will respond. Along with the continuous freezing, the impedance of the electrodes mounted at 9 and 12 mm from the tip also jumps to the insulation region when the ice front occurs. These results indicate that the cooling power produced by the present cryoprobe is strong enough. The impedance of electrodes positioned 15 mm from the tip show no evident increases during freezing. When the ice ball stopped growing, the liquid nitrogen supply was shut off. It was found that the impedance decreased rapidly at these electrodes along with the thawing of the ice ball. There is a large impedance fluctuation at the electrode that is 9 mm from the tip (see Fig. 13). This is because a certain crack has occurred inside the ice ball, and the electrode there may separate from the ice. This may suggest a new way to evaluate cracks in frozen biomaterials during rewarming. The impedance returned to a normal level, when the ice ball disappeared.

Experimental results in the phantom gel are given in Fig. 14, which are almost the same as in Fig. 13. The impedance also quickly increased when the ice ball arrived and decreased when the ice ball disappeared. The growth rate of the ice ball is slower in phantom gel than in water, and the size of the ice ball is bigger in the former case because the impedance of the electrode placed at 15 mm jumps to an insulation region. The difference was due to a variation in thermal characteristics between water and phantom gel. To test the sensitivity of the impedance response, we intentionally shut off the supply of liquid nitrogen for a short period during the freezing. Then as indicated in Fig. 14, the impedance quickly goes down with an increase of temperature. Figures 15 and 16 give the overall ICR and partial ICR in phantom gel experiments. From Fig. 15, it is clear to show five jumps of ICR, along with the arrival of the ice ball at the position of the electrodes during freezing. Figure 16 depicts the partial ICR when liquid nitrogen was shut off for a short while. It was seen that the ICR represents the temperature change with a little decrease. Contrasted with the DLFI curve shown as Fig. 14, the ICR image can be regarded as another efficient method to detect the ice front growth along the cryoprobe.

4. DISCUSSION

The DLFI of biological materials during freezing can provide useful information for ice formation and thawing, which is critical information to

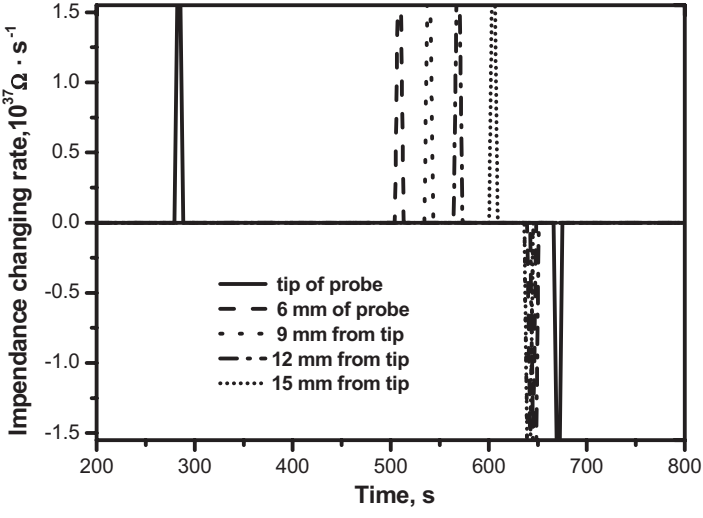

Fig. 15. Overall ICR in phantom gel experiment.

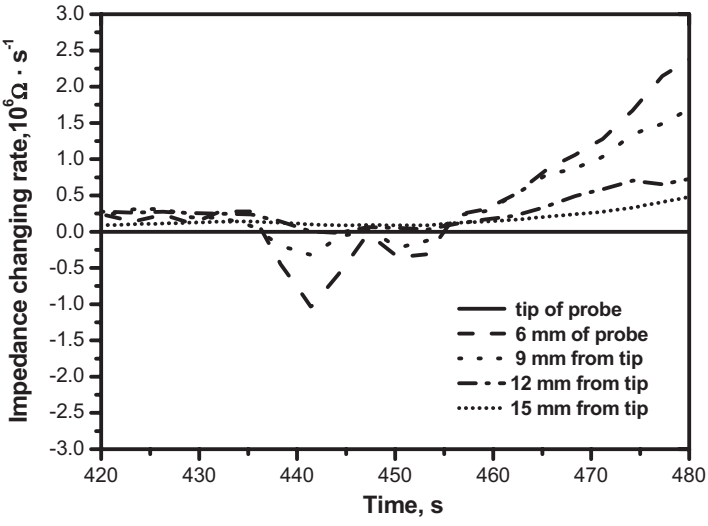

Fig. 16. Partial ICR during the period of temperature increase in phantom gel experiment.

assess the freezing damage of biological materials. Contrasted to the DLFI, the ICR is an alternative way to evaluate the freezing behavior of biological materials, especially around the phase-change region. Shown in Fig. 8, the ICR has a sudden drop when the phase change occurs and the latent heat is released. It may possibly reveal the relation between ice formation and cell damage. The ICR method may present an efficient tool to study in detail the phase-change problem, which will be the focus of our following work.

One of the main difficulties encountered in cryosurgery is the uncertainty in the freezing extent and depth of the treated tissue. The DLFI and ICR methods investigated in this study can quickly monitor the ice front by the impedance jump of needle electrodes mounted along the cryoprobe (see Figs. 14 and 15). Besides, these two methods are also useful to monitor the temperature change of the probe tip. The response is rapid and direct, and the values of the DLFI and ICR decrease immediately when the temperature of the probe increases.

Although the depth of the ice front inside biological tissue cannot be monitored, the present method can provide essential complementary information to traditional methods like ultrasonic, MRI, and CT. The large impedance variation between frozen and unfrozen tissue, for example, prevents absolute imaging in the traditional EIT. The DLFI and ICR methods proposed in this study would alleviate this problem to some extent

during cryosurgery. Although the initial results presented are encouraging, they should not overshadow the fact that many fundamental obstacles still need to be overcome in future studies. For example, the needle electrodes are discretely fixed along the cryoprobe in this study, which is not the most appropriate way in clinics. To solve this problem, it is possible that a special thin film can be placed around the exterior of the probe in applications with electrodes fabricated inside it. It should be emphasized that the development of this measurement system is merely the first step in the design of what may eventually prove to be a simple, inexpensive supplement to existing methods for cryosurgical monitoring.

5. CONCLUSION

Due to obstacles in using conventional monitoring techniques, further development of cryosurgery is in urgent need of a simple, flexible, and inexpensive monitoring method. This study has been performed to test the DLFI method to detect the ice front to aid in the eventual creation of an EIT-based cryosurgical monitoring system. The DLFI for some biological materials (fresh pork, fresh rabbit muscle and organ), subject to freezing under different cooling temperatures, was investigated and found very useful for predicting ice formation and thawing. Besides, the ICR method proposed in this paper, may provide a powerful way to study the phase-change problem. The feasibility of DLFI and ICR methods to detect ice front propagation in cryosurgery was demonstrated by placing needle electrodes at the exterior of a cryoprobe, and *in vitro* experiments were also performed on the water and phantom gel. The experimental tools developed in this study will be used in the near future to develop a simple, inexpensive system intended specifically for cryosurgical monitoring.

ACKNOWLEDGMENT

The authors are grateful for funding support from the "One Hundred Scientists Program" and the Innovation Funding by the Chinese Academy of Sciences.

REFERENCES

1. P. Mazur, *Science* **168**:939 (1970).
2. D. M. Otten and B. Rubinsky, *IEEE Trans. Biomed. Eng.* **47**:1376 (2000).
3. L. I. Poletaev, Y. V. Makeev, and V. A. Mikhailov, *Med. Prog. Thro. Tech.* **18**:91 (1992).
4. Y. Kinouchi, T. Iritani, T. Morimoto, and S. Ohyama, *Med. Biol. Eng. Comput.* **35**:486 (1997).
5. B. M. Eyuboglu, T. C. Pilkington, and P. D. Wolf, *Phys. Med. Biol.* **39**:1 (1994).

6. B. K. van Kreel, *Med. Biol. Eng. Comput.* **39**:551 (2001).
7. C. J. Slager, A. C. Phaff, C. E. Essed, N. Bom, J. H. Schuurbiers, and P. W. Serruys, *IEEE Trans. Biomed. Eng.* **39**:411(1992).
8. B. K. van Kreel, N. Reyven, and P. Soeters, *Med. Biol. Eng. Comput.* **36**:337(1998).
9. J. Jossinet, *Med. Biol. Eng. Comput.* **34**:346 (1996).
10. P. J. Pivert, P. Binder, and T. Ougier, *Cryobiology* **14**:245 (1977).
11. M. M. Radai, S. Abboud, and B. Rubinsky, *Cryobiology* **38**:51 (1999).
12. S. Kun and R. Peura, *IEEE Trans. Biomed. Eng.* **47**:163 (2000).
13. I. Schneider, *Proc. 18th Ann. Int. Conf. IEEE Eng. Med. Bio. Soc.* (Amsterdam, 1996), pp. 1934–1935.
14. K. Takada, S. Sugita, R. Ikeuchi, N. Okuda, and T. Fujinami, *Med. Prog. Thro. Tech.* **19**:187 (1993).
15. G. A. Sandison, M. P. Loye, J. C. Rewcastle, L. J. Hahn, J. C. Saliken, J. G. McKinnon, and B. J. Donnelly, *Phys. Med. Biol.* **43**:3309 (1998).
16. P. Laugier, J. Lefaix, and G. Berger, *Proc. IEEE Ultrasonics Symp.* (1998), pp. 1337–1340.
17. F. Parivar, H. Hricak, K. Shinohara, J. Kurhanewicz, D. B. Vigneron, S. J. Nelson, and P. R. Carroll, *Adult Urology* **48**:594 (1996).
18. S. Rush, J. A. Abildskov, and R. McFee, *Circ. Res.* **12**:40 (1963).
19. T. E. Cooper and W. K. Petrovic, *J. Heat Transfer.* **96**:415 (1974).
20. H. Budman, A. Shitzer, and S. D. Giudice, *J. Biomech. Eng.* **108**:42 (1986).
21. B. Rubinsky and G. Onik, *Int. J. Refrig.* **14**:190 (1991).
22. G. R. Pease, B. Rubinsky, J. C. Gilbert, and A. Arav, *J. Biomech. Eng.* **117**:59 (1995).